

PCCP

Accepted Manuscript



This is an *Accepted Manuscript*, which has been through the Royal Society of Chemistry peer review process and has been accepted for publication.

Accepted Manuscripts are published online shortly after acceptance, before technical editing, formatting and proof reading. Using this free service, authors can make their results available to the community, in citable form, before we publish the edited article. We will replace this *Accepted Manuscript* with the edited and formatted *Advance Article* as soon as it is available.

You can find more information about *Accepted Manuscripts* in the [Information for Authors](#).

Please note that technical editing may introduce minor changes to the text and/or graphics, which may alter content. The journal's standard [Terms & Conditions](#) and the [Ethical guidelines](#) still apply. In no event shall the Royal Society of Chemistry be held responsible for any errors or omissions in this *Accepted Manuscript* or any consequences arising from the use of any information it contains.

The vibrational spectroscopy of the coordinated azide anion; a theoretical study.

Eliano Diana^a, Karl Gatterer^b and Sidney F.A. Kettle^c.

^a Dipartimento di Chimica, Università di Torino, via P. Giuria 7, 10125 Torino, Italy, e-mail:

eliano.diana@unito.it

^b Institut für Physikalische und Theoretische Chemie, Technische Universität Graz,

Stremayrgasse 9, A-8010 Graz, Austria, e-mail: gatterer@tugraz.at

^c Department of Chemistry, University of East Anglia, Norwich NR4 7TJ, U.K.

Tel:+441263731179; e-mail: s.kettle@uea.ac.uk

KEYWORDS

Azide, vibrational spectroscopy, DFT, model system.

ABSTRACT

The vibrational behaviour of the azide anion in a variety of environments has been examined by DFT methods. The frequency is sensitive to polar, dipolar and quadrupolar fields. The frequency is also dependent on the metal to which it is bonded and thus to the details of that bonding. Several azides within one molecule can be strongly vibrationally coupled, a coupling which

carries with it a transfer of spectral activity. It is suggested that whilst absolute vibrational frequencies carry little immediately accessible information, a combination of infrared and Raman data for the antisymmetric stretch region might give limited structural insights.

Introduction

The azide anion is a ligand that shows a remarkable versatility in the range of coordination complexes that it forms. As a terminal ligand, the coordinated metal can be either co-linear with the ligand axis or at an angle to it. As a simple bridging ligand, the bridge can involve a single terminal N atom, bonded to two metal atoms, or the N at either end of the ligand can bond to different metal atoms. Surprisingly commonly, however, it is incorporated in a more complicated manner, particularly when other ligands of some complexity are involved¹. The basics of the vibrational spectroscopy of the azide anion have long been well understood², as have its characteristics in coordination compounds³. In that all azide complexes show an asymmetric azide stretching vibrational mode at ca 2100 cm⁻¹ which has strong infrared activity, there have been many attempts to relate the frequency (and, to a lesser extent, the intensity) of this spectral feature to the coordination mode of the azide. No clear picture has emerged. Although a consistent pattern of behaviour has been found between closely related members of a series, no significant transferability seems to exist. Conversely, an infrared frequency of 2075cm⁻¹ is one that seems consistent with almost any mode of azide coordination. The situation is well indicated by quotations from publications some forty years apart^{4,5}:- one should avoid making comparisons between markedly different complexes, that is, between complexes which are of different geometry or which contain different metal atoms in different oxidation states. Moreover, in most cases, the degree of coordination of the azide ligand, that is, whether it is monocoordinate or bridging, cannot be established solely from a consideration of infrared data⁴ and: the $\nu_{as}(N_3)$ of

the azido group in azido–Cd(II) could help in predicting the bonding coordination mode of the bridged azide, but it cannot be used as a diagnostic tool to elucidate for certainty the bonding mode of the azide groups in these complexes⁵.

There are other vibrational modes of the azide, notably a symmetric stretch at ca 1400 cm⁻¹ and deformation modes at ca 650 cm⁻¹ but these have been little studied; their identification is problematic. Relatively few Raman data (which might explore the 1400 cm⁻¹ mode) are available – whilst the symmetric stretch and the deformation modes lack spectral dominance and occur in spectral regions commonly rich with other features.

The complexity of the vibrational spectroscopy of the complexed azide anion is in contrast to that of the cyanide, CN⁻, ligand. For this ligand a rather consistent picture has been generally accepted, in which metal-ligand π bonding (into ligand antibonding orbitals) is held to be of importance; as a bridging ligand the so-called kinematic effect was accepted as an explanation of the observed behaviour⁶. However, there were some data which could not be understood in terms of this model, and this led us to undertake a detailed experimental and, particularly, theoretical, study of the vibrational spectroscopy of the cyanide ligand⁷. The conclusions were quite surprising, in view of the simplicity of the ligand. The dominant effect controlling the vibrational frequency of a coordinated cyanide group is that of the electrostatic field to which it is subjected, be a single metal atom or several involved. Kinematic and π bonding are but minor effects. The theoretical work involved was largely based on DFT calculations (often on model systems) but normal coordinate analyses (including some on the outputs of the DFT calculations) also featured. The success of this approach led us to the present DFT study of the vibrational spectroscopy of the azide anion. DFT methodology has previously been applied to azides⁸, and whilst vibrational data have been reported, these have never been the

focus of attention. The present work is the first to report on the vibrational spectroscopy of the azide ligand and their changes on coordination to a metal.

Calculations

The computational modelling of azides has been done by a DFT approach, using the hybrid functional B3LYP and the extended 6-311++g(d,p) basis set. All the models examined have been optimized to a minimum of energy (checked by exploring vibrational frequencies) and harmonic vibrational frequencies computed. The effect of charges and electric fields on N_3^- have been evaluated with the azide in fixed orientations. Additionally, we have varied the position of the azide group within model species and report the consequential vibrational frequency changes. All calculation have been performed with the Gaussian 09 package⁹.

Results

As a marker, we carried out an optimization of the isolated azide anion. The anion was calculated to be of $D_{\infty h}$ symmetry, with $d(\text{N-N}) = 1.183 \text{ \AA}$ and unscaled vibrational frequencies of 2076 (Σ_u), 1351 (Σ_g) and 628 (Π) cm^{-1} . The bond length may be compared with a typical experimental value of $d(\text{N-N}) = 1.162 \text{ \AA}$ (in lithium azide¹⁰). In the present work we prefer to present unscaled frequencies since we believe that this gives a better indication of the effect of the variables that we consider.

Model systems

In our study of the cyanide anion it was found that the calculated vibrational frequency was very sensitive to the magnitude and position of an adjacent positive charge⁷. This is true for the azide anion as well. Figure 1 shows the variation of the frequencies exhibited by the azide

anion in the presence of a variable positive charge placed 2.02 \AA (the observed separation in $[\text{CaN}_3]^+$) from the nearest nitrogen and coaxial with the anion. The charge was varied from 0 to 1.0, so that the overall charge of the system varied from -1 to 0. Not surprisingly, only the dipolar modes were sensitive to the charge variation. The frequency of Σ_u increased approximately linearly with the charge, with a maximum change of ca 60 cm^{-1} . The changes to the Π mode were more dramatic. Its frequency increased in a non-linear fashion, with a change of ca 50 cm^{-1} for a charge of +0.75. However, further increase of the charge to +1.0 caused the frequency to drop to below its original value. The frequency of Σ_g varied little with charge variation. These data indicated a clear sensitivity of azide frequencies to electrostatic aspects of its environment. We therefore investigated the consequences of an applied electrostatic dipole and an applied electrostatic quadrupole. It was only possible to explore a small electrostatic dipole along the molecular axis; instability and imaginary frequencies occurred for those larger than indicated in Table 1. Here the antisymmetric stretch was least affected and the symmetric the greatest. Much larger changes were found when the dipole is perpendicular to the molecular axis (Table 2), although now the symmetric mode varies little. Both the antisymmetric stretch and deformation modes showed considerable sensitivity, with the latter significantly split. A quadrupolar field perpendicular to the molecular axis caused but small frequency changes, although the deformation modes were split (Table 3). When applied along the molecular axis, the consequences were much greater (Table 4). The symmetric stretch frequency shows a great sensitivity and, *in extremis*, appears in a totally different spectral region.

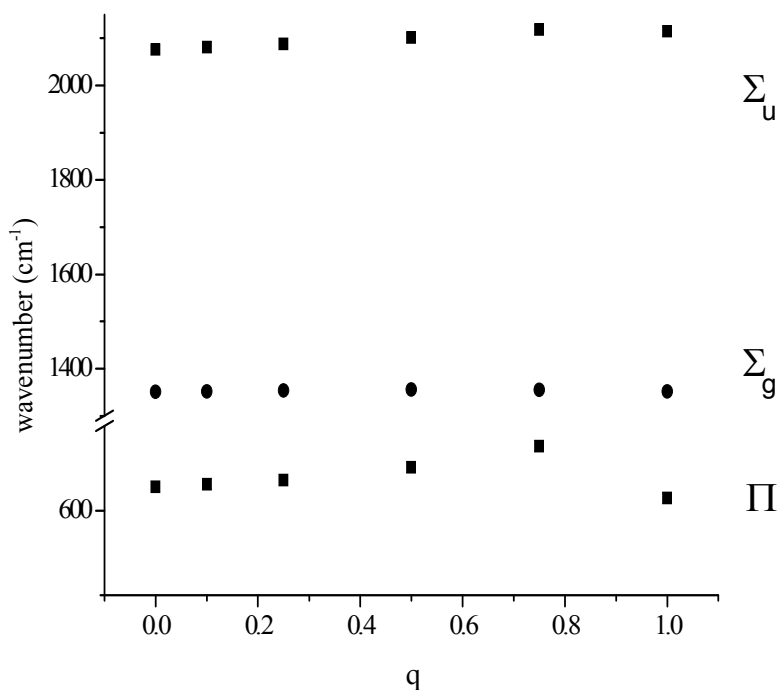


Figure 1 Variation of calculated azide frequencies (cm⁻¹) for a N³⁻...q system, with variation of an adjacent charge q.

The antisymmetric stretch is sensitive, but less so until the field becomes great - when the frequency sensitivity increases. The deformation modes are not greatly affected until, again, the field becomes great. Almost certainly, the quadrupole limit that we have studied is unrealistic – an attempt to increase it further led to imaginary frequencies. However, the sensitivities that we report are surely real.

	0	0.04	0.045	0.048
$\Sigma_u(\nu_{as})$	2076	2079	2078	2078

$\Sigma_g(\nu_s)$	1351	1342	1340	1339
Π	628	642	639	637

Table 1 Effect on vibrational frequencies (cm^{-1}) of a dipole field applied to N_3^- (in a.u.) along the molecular axis.

	0	0.04	0.05	0.06
$\Sigma_u(\nu_{as})$	2076	2052	2035	2010
$\Sigma_g(\nu_s)$	1351	1350	1349	1348
Π	628	615	607	597
Π	628	590	568	540

Table 2 Effect on vibrational frequencies (cm^{-1}) of a dipole field applied to N_3^- (in a.u.) perpendicular to the molecular axis.

	0	0.0001	0.0002	0.0003	0.0005	0.0007
$\Sigma_u(\nu_{as})$	2076	2075	2074	2073	2071	2068
$\Sigma_g(\nu_s)$	1351	1350	1349	1347	1352	1334
Π	628	636	638	635	636	634
Π	628	631	634	632	599	531

Table 3 Effect on vibrational frequencies (cm^{-1}) of a quadrupole field applied to N_3^- (in a.u.) perpendicular to the molecular axis.

	0	0.0001	0.0002	0.0003	0.0005	0.0007
$\Sigma_u(\nu_{as})$	2076	2075	2068	2054	2006	1926
$\Sigma_g(\nu_s)$	1351	1339	1301	1234	979	288
Π	628	639	634	612	504	195

Table 4 Effect on vibrational frequencies (cm^{-1}) of a quadrupole field applied to N_3^- (in a.u.) parallel to the molecular axis.

We have modelled two possible bridging modes of the azide ligand. In the first, the azide is perpendicular to the metal-metal axis (here, charge-charge axis), q1-N(2)-q2 subtending an angle of 107° , the charges being equal and with maximum values of $+\frac{1}{2}$. The charges were both separated from the terminal N, N(1), by 2.0 Å. the Σ_u and Σ_g frequencies increase by a few wavenumbers with charge increase: it is the Π which shows major changes, both splitting, by over 30 cm^{-1} , and increasing in value by up to 40 cm^{-1} . The behaviour is shown in Figure 2.

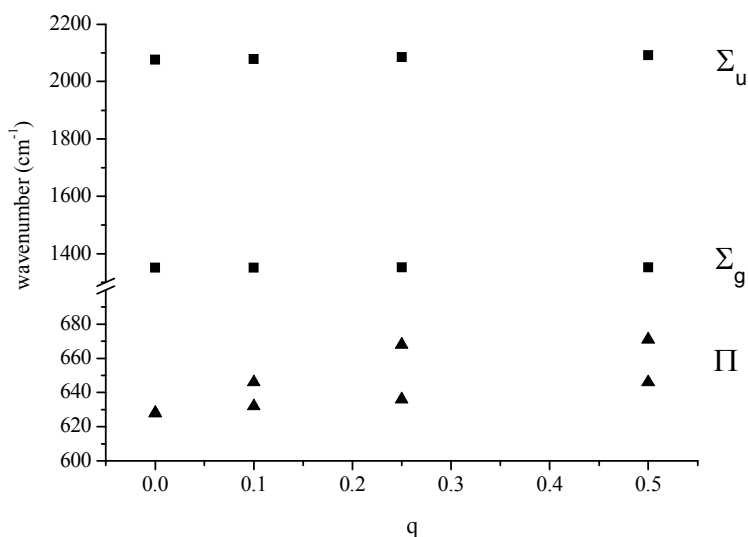


Figure 2 Variation of calculated azide frequencies with variation of two equal charges perpendicular to the anion axis (modelling an azide bridging two metal atoms)

The second possible bridging mode of the azide ligand may be modelled by placing identical variable charges at either end of the anion, at a fixed separation (2.0 \AA was chosen) from and co-linear with it. The variations shown in Figures 3 and 4 were obtained. Whilst the frequency of the Σ_g vibration changes little with variation of the charge, both the Σ_u and Π show considerable sensitivity, the latter particularly so. When the charges increased to +1.5 (from zero) the Π frequency doubled. The effect on Σ_u maximised at a charge of +0.8 (with an increase of ca 80 cm^{-1}). The N-N bond-length variation was somewhat surprising; an initial small contraction (maximising at a charge of +0.3) was followed by an extension which approached 1% at a charge of +1.5.

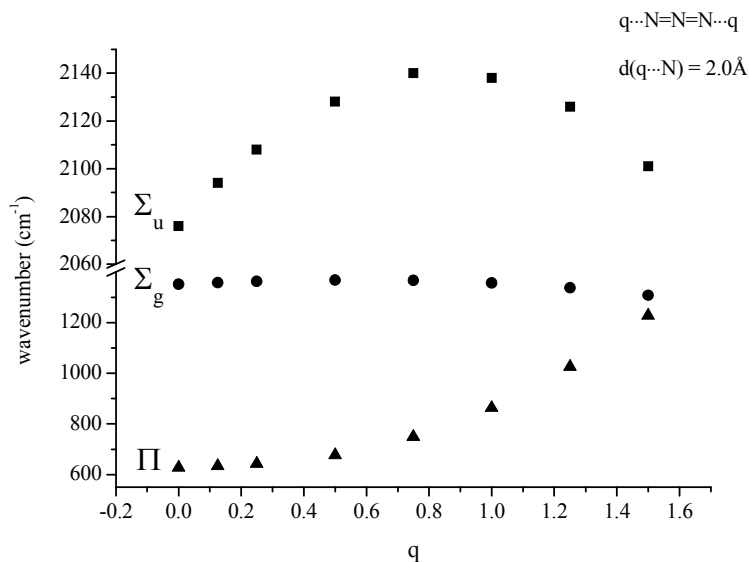


Figure 3 Variation of calculated azide frequencies (cm⁻¹) with variation of two equal charges, one at each end of the anion and co-linear with it (modeling an azide bridging two metal atoms).

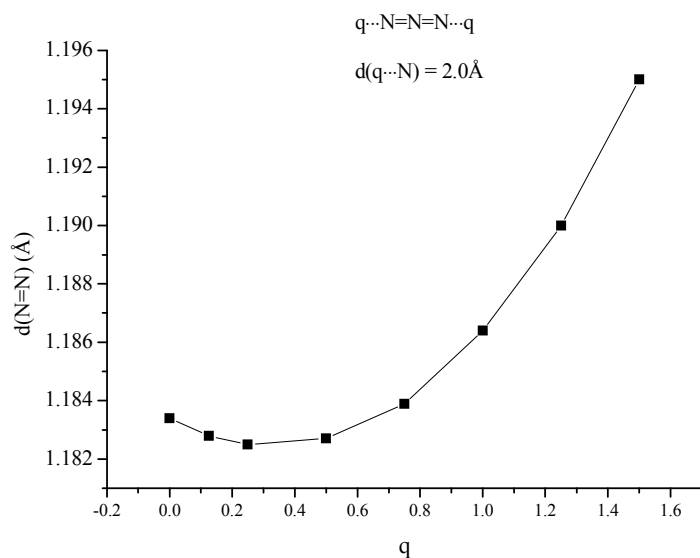


Figure 4 Variation of N-N bond length (Å) with variation of two equal charges, one at each end of the anion and co-linear with it (modeling an azide bridging two metal atoms).

Metal-containing systems

It has been shown so far, that azide frequencies are sensitive to the charge and multipolar nature of the azide local environment. This conclusion makes understandable the failure to find clear correlations between observed vibrational frequencies and the mode of bonding of the azide anion. Such correlations are dependent of the absence of any charge-sensitivity. We then investigated metal-specific effects. Initially, we studied the interaction between a chosen metal atom, or set of atoms, with the azide ligand without any complication imposed by additional ligands. We first made a detailed study of the bonding between simple metal ions and the azide ligand in an ‘end-on’ arrangement where two different geometries are possible. Either the metal is co-linear with the azide, in a $C_{\infty v}$ arrangement, or it is at an angle to it, the symmetry dropping to C_s . The latter geometry is the more important because it is also that commonly found when an azide bridges metal atoms. Some comments on the interactions which determine whether a $C_{\infty v}$ or C_s arrangement is adopted by a MN_3 unit (with $M = Cu$) will be found in Appendix 1.

Table 5 gives the results for DFT calculations on $M(I)$ azides of first row transition metals and adjacent cations. It is clear that there are specific bonding effects; generally the $M-N-N$ angle tends to decrease with increasing d electron count. However, the Mn compound, with the lowest calculated metal charge, is also linear. Again, the linear species tend to have the longest $M-N_3$ bonds – but the linear Mn compound has the shortest.

There seems to be no strong dependence of frequency on any of the possibly relevant molecular quantities, such as metal or nitrogen atom charge or on bond lengths (although a correlation with bond length differences has been suggested for some species)³. The data support the suggestion that both electrostatics and bonding are of importance in determining the

vibrational frequency exhibited by a coordinated azide ligand. General patterns are not to be expected.

	K	Ca	Sc	Ti	V	Cr	Mn	Fe	Co	Ni	Cu	Zn
ν_{as}	2167	2220	2251	2241	2191	2205	2225	2170	2178	2165	2165	2161
ν_s	1397	1427	1456	1436	1381	1399	1430	1342	1375	1334	1345	1336
π	654	679	600	647	586	610	575	651	602	647	649	620
π	654	679	600	647	519	569	575	558	571	552	575	580
	287	387	467	426	425	447	428	447	457	454	444	370
	87	125	98	124	95	103	39	129	115	137	145	135
	87	125	98	124			39					
$q_{(M)}$	0.955	0.863	0.617	0.584	0.663	0.647	0.564	0.640	0.624	0.634	0.687	0.663
$q_{(N1)}$	-0.809	-0.879	-0.769	-0.729	-0.691	-0.673	-0.674	-0.660	-0.643	-0.664	-0.687	-0.700
$q_{(N2)}$	0.188	0.219	0.241	0.237	0.203	0.204	0.232	0.193	0.195	0.191	0.186	0.189
$q_{(N3)}$	-0.334	-0.203	-0.090	-0.092	-0.175	-0.179	-0.122	-0.173	-0.176	-0.162	-0.186	-0.152
M-N-N	180	180	180	180	149	143	180	131	138	127	124	124
N-N-N	180	180	180	180	175	176	180	174	176	174	174	176
d(M-N)	2.379	2.138	1.913	1.893	1.901	1.883	1.802	1.846	1.799	1.816	1.845	1.943

Table 5 Vibrational frequencies (cm^{-1}), atomic charges and molecular parameters (distances are in Å, angles in degrees) calculated by the DFT method for some $M(I)N_3$ complexes

Table 6 shows the results of calculations for $[M(II)N_3]^+$ cations. Linearity is rare and occurs for those with the largest calculated metal charge; these are also the species with the highest calculated asymmetric stretching frequency. Noteworthy is the Cu(II) compound. It has, by far,

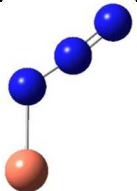
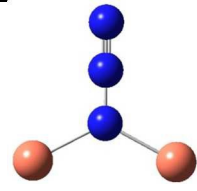
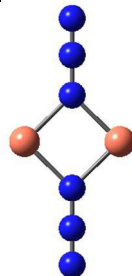
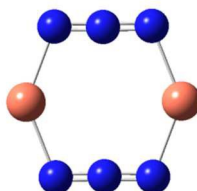
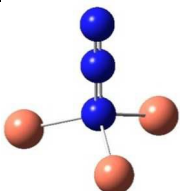
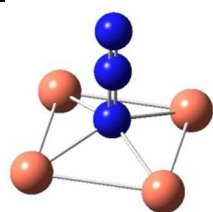
the lowest antisymmetric frequency and also the lowest calculated metal charge. The next lowest metal charge is exhibited by Ni, which also has the next lowest antisymmetric frequency. It would seem that these calculations show electrostatic effects beginning to dominate bonding.

	Ca	Sc	Ti	V	Cr	Mn	Fe	Co	Ni	Cu	Zn
ν_{as}	2260	2270	2238	2226	2230	2192	2195	2291	2086	1862	2154
ν_s	1416	1399	1279	1374	1433	1234	1285	1571	1295	1338	1239
π	665	579	520	538	560	570	568	663	594	568	620
π	665	579	501	517	521	485	483	507	476	459	527
	473	512	442	491	494	460	476	500	443	353	429
	154	141	115	81	95	127	103	122	113	109	183
	154	141									
$q_{(M)}$	1.744	1.478	1.313	1.374	1.341	1.179	1.166	1.111	1.020	0.986	1.329
$q_{(N1)}$	-0.991	-0.829	-0.719	-0.714	-0.644	-0.579	-0.564	-0.502	-0.412	-0.328	-0.634
$q_{(N2)}$	0.234	0.249	0.239	0.229	0.213	0.218	0.213	0.199	0.180	0.155	0.178
$q_{(N3)}$	-0.017	0.102	0.166	0.111	0.090	0.182	0.185	0.192	0.212	0.186	0.127
M-N-N	180	180	170	164	159	151	152	154	141	139	120
N-N-N	180	180	178	178	177	176	176	177	175	175	171
d(M-N)	2.020	1.853	1.774	1.801	1.785	1.732	1.719	1.729	1.733	1.879	1.872

Table 6 Vibrational frequencies (cm^{-1}), atomic charges and molecular parameters (distances are in Å, angles in degrees) calculated by the DFT method for some $M(\text{II})\text{N}_3$ complexes

In Tables 5 and 6, copper azides stand apart. In Table 5, the Cu(I) compound, *inter alia*, has a remarkable balancing of calculated internal charges; its unique position in Table 6 has already been commented upon. We chose this metal for an investigation into other aspects of azide

coordination, the bonding of more than one azide and azide as a bridging ligand. Table 7 shows the results of calculations on azide complexes of Cu(I) and Cu(II), along with the relevant data from either Table 5 or 6. Several things are evident from this Table. First, when there are two azide groups, all of the infrared intensity is confined to one of the resultant paired modes unless the molecular symmetry is very low. Second, this infrared active mode may be that at higher frequency or that at lower, there seems to be no evident rule. Thirdly, a charge effect seems to be operating, in that the frequencies of Cu^+ species are higher than those of Cu^{2+} , the infrared intensities are also greater. Fourthly, the frequencies of bridging azides are not very sensitive to the number of metal atoms bridged for an unchanged orientation of the azide. It is not possible to make

						
CuN_3	$[\text{Cu}_2\text{N}_3]^+$	$\text{Cu}_2(\text{N}_3)_2$	$\text{Cu}_2(\text{N}_3)_2$	$[\text{Cu}_3\text{N}_3]^{2+}$	$[\text{Cu}_4\text{N}_3]^{3+}$	
sym	C_s	C_{2v}	D_{2h}	D_{2h}	C_{3v}	C_{4v}
ν_{as}	2165	2245	2229(0), 2212(2045)	2158(1686), 2062(0)	2265	2264
ν_{s}	1346	1250	1380(0), 1368(196)	1360(0), 1357(1)	1057	947
π	649	728	655(14), 654(0)	676(0), 672(10)	625	593

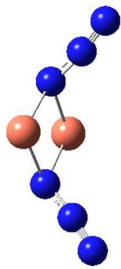
π	575	560	583(11), 580(0)	598(8), 596(0)	625	593
						
	$[\text{CuN}_3]^+$	$[\text{Cu}_2\text{N}_3]^{3+}$	$[\text{Cu}_2(\text{N}_3)_2]^{2+}$	$[\text{Cu}_2(\text{N}_3)_2]^{2+}$	$[\text{Cu}_3\text{N}_3]^{5+}$ Not optim.	$[\text{Cu}_4\text{N}_3]^{7+}$ Imaginary freq.
sym	C_s	C_{2v}	C_{2v}	D_{2h}	C_{3v}	C_{4v}
ν_{as}	1862	1974	2156(29), 2151(51)	1892(0), 1884(185)	2245	
ν_s	1338	1029	1135(47), 1128(123)	1389(0), 1383(1)	1105	
π	568	598	608(7), 604(0)	624(0), 611(2)	573	
π	459	421	575(3), 558(5)	571(7), 494(0)	567	

Table 7 Calculated vibrational frequencies (cm^{-1}) for some copper-azide complexes (upper, Cu^+ , lower, Cu^{2+}). Where relevant, infrared intensities (KM/mole) are given in brackets

meaningful comparisons between the data in Table 7 and experimental results. The data in Table 7 are unscaled, omit the other ligands which are part of the experimental data (and which will influence the formal charge on the Cu) and ignore the fact that many of the relevant compounds are polymeric. However, we note that Agrell³ reports data covering the range 2125-

2030 cm^{-1} for simple species and more recent data fall in this range (for example¹¹, 2045 cm^{-1}). Data for single N-bonded $\text{Cu}_2(\text{N}_3)_2$ bridge species show a similar range, (2137-2040 cm^{-1})¹². Data on doubly N-bonded $\text{Cu}_2(\text{N}_3)_2$ bridge species are more limited^{12e, 13} and are near 2055 cm^{-1} . However, this figure is surely deceptive in that one species with both types of bridge has frequencies at 2110 and 2115 cm^{-1} ¹⁴. The data in Table 7 show the extreme vibrational frequency sensitivity of bare Cu-azide systems to the details of the geometric structure and electronic configuration. Experimental data indicate that addition of other ligands or increase in molecular unit size does nothing to simplify the situation.

We have considered in more detail the question of how, given a stoichiometry, the calculated vibrational frequencies vary with geometrical arrangement. Given that bonding will be particularly dependent on the metal chosen, we have opted for a system that will be rather ionic. This has the additional advantage that polar effects will not significantly be in competition with bonding and so should enable a second assessment of the importance of electrostatic effects. The system that we have chosen is, inevitably, somewhat artificial. It is $\text{Na}_2(\text{N}_3)_2$. The basic configuration is shown in Figure 5; it consists of two coplanar azides interleaved by two sodium cations. In a first set of calculations the distance between the central

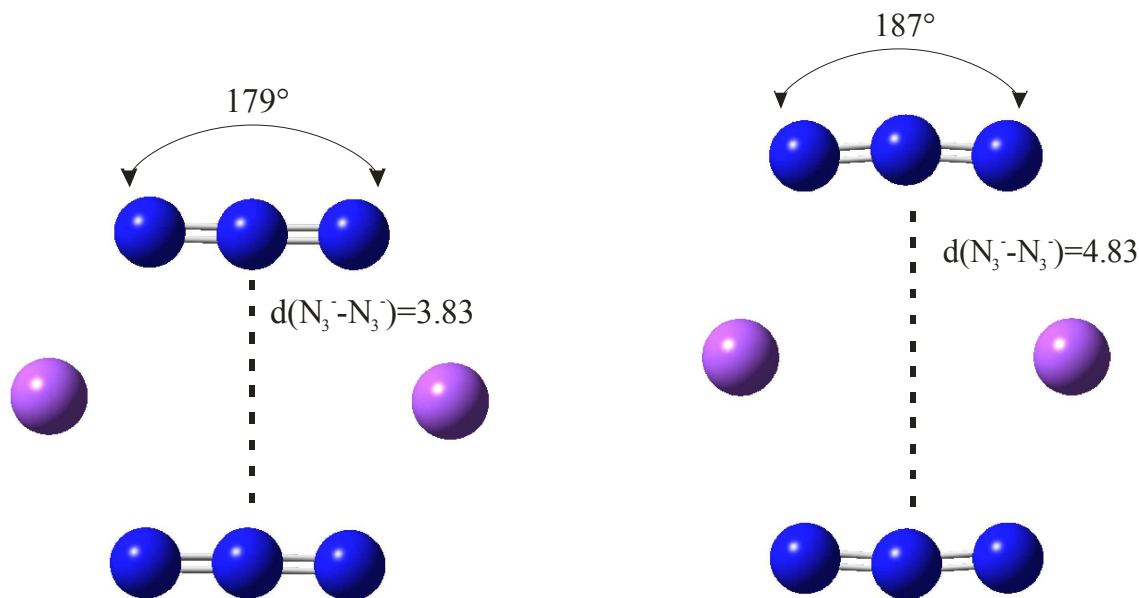


Figure 5 The limiting arrangements of $\text{Na}_2(\text{N}_3)_2$ considered in the text. The $\text{N}_3^- - \text{N}_3^-$ distances (\AA) were varied and all other geometrical parameters optimised.

nitrogens of the azides was fixed and all other quantities optimised. The central N-N distance was varied from 3.83 to 4.83 \AA , when the N-N-N angle of each azide decreased from 179 to 187°. The results are shown in Figure 6. Both antisymmetric and symmetric frequencies are sensitive to the inter-azide separation. The symmetric modes appear uncoupled in that no splitting occurs, although the frequency varies (indicating the relevance of electrostatic effects). The antisymmetric modes couple strongly, with a coupling which is not strongly dependent on inter-azide separation. However, one antisymmetric mode is strong in the infrared, the other is calculated to have a zero intensity. Hence the infrared spectra of double azide bridges may be deceptively simple. The Raman are also surprising. The antisymmetric combination of antisymmetric stretches is invariably calculated to be the mode with greatest Raman intensity, greater than the sum of the intensities of the symmetric stretches. In a second set of calculations,

in the configuration of Figure 5 with the inter-azide distance fixed at 3.83\AA , the azides were rotated relative to each other, with the torsion angle varied in steps of 15° , as indicated in Figure 7. The results are shown in Figure 8. Both symmetric and antisymmetric modes show a frequency dependence; the latter behave as expected for dipolar behaviour – the coupling between the vibrators decreases to zero at a torsion angle of 90° . By this angle the antisymmetric combination of antisymmetric stretches has become very visible in the infrared but has lost Raman intensity; with a torsion greater than 30° , its intensity is less than the summed intensity of the symmetric stretches (at 30° they are calculated to be equal). Full details are given in Table 8.

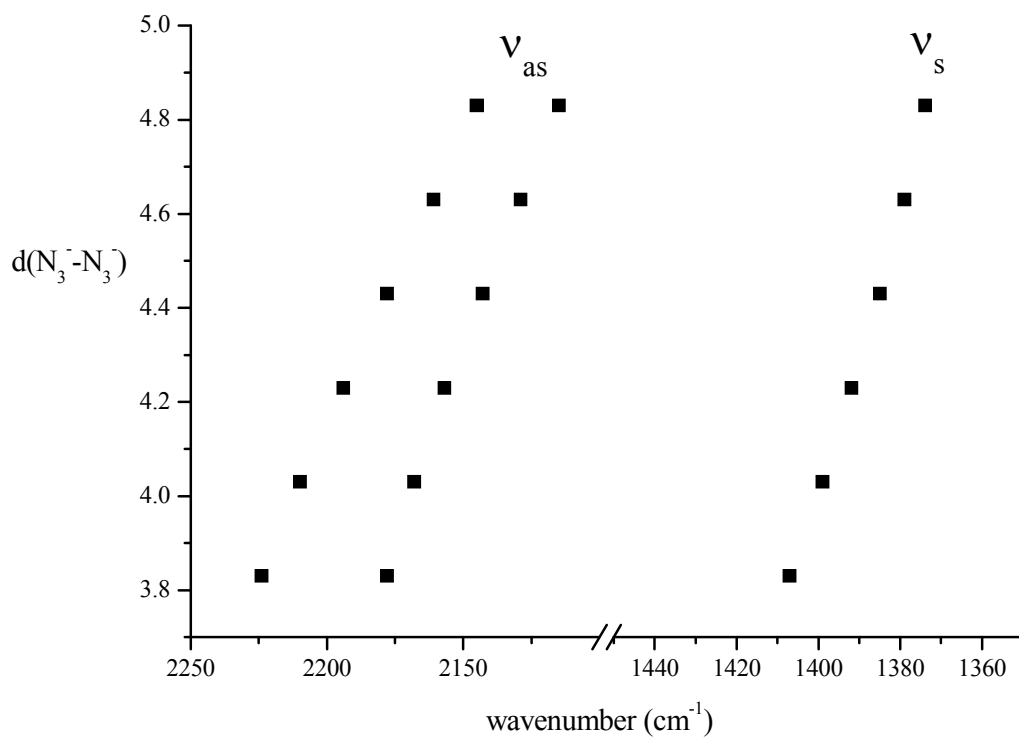


Figure 6 Variation of azide stretching frequencies (cm⁻¹) as the N₃⁻ - N₃⁻ separation (Å) is changed, for the arrangement shown in Figure 5

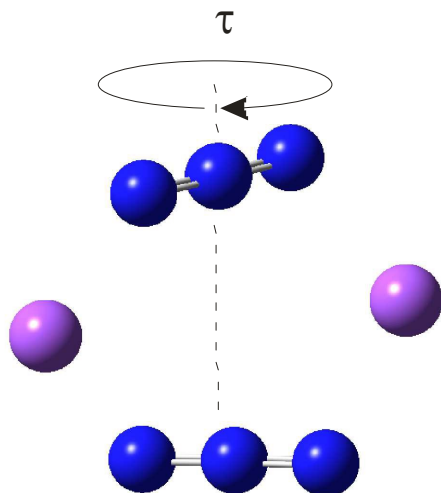


Figure 7 Torsional variation (of τ in steps of 15°) of $\text{Na}_2(\text{N}_3)_2$ with a central $\text{N}\cdots\text{N}$ separation of 3.83\AA

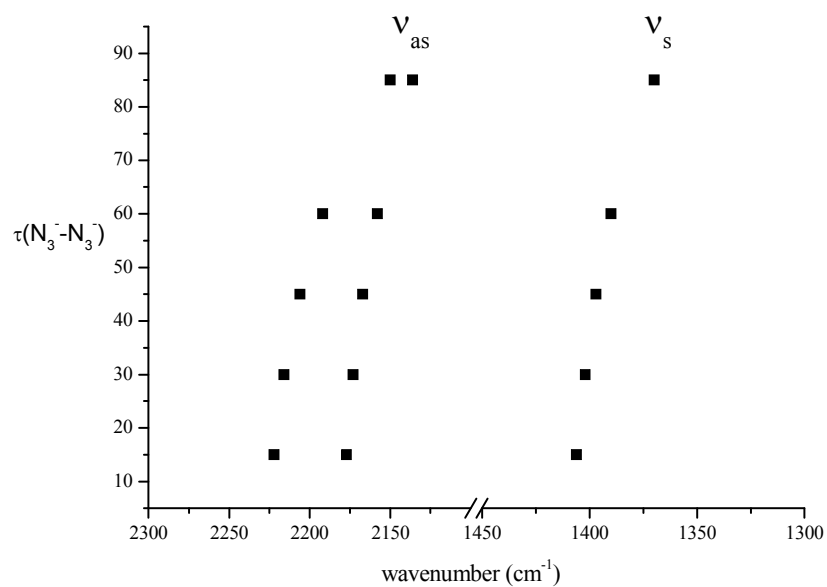


Figure 8 Variation of azide stretching frequencies (cm^{-1}) for the set of structures of Figure 7

	Azide-Azide shift						Azide-Azide torsion					Azide-Azide slip				
	0	0.2	0.4	0.6	0.8	1.0	15	30	45	60	85	0.2	0.4	0.6	0.8	1.0
ν_{as}	2224 (1602,0)	2210 (1613,0)	2194 (1626,0)	2178 (1643,0)	2161 (1668,0)	2145 (1702,0)	2222 (1582,0)	2216 (1526,0)	2206 (1438,0.1)	2193 (1320,0.2)	2150 (1023,0.6)	2226 (1609,0)	2224 (1627,0.0)	2225 (1652,0.0)	2222 (1667,0.0)	2221 (1697,0.0)
ν_{as}	2178 (0,41)	2168 (0,43)	2157 (0,54)	2143 (0,66)	2129 (0,85)	2115 (0,114)	2177 (21,39)	2173 (82,36)	2167 (177,32)	2158 (298,27)	2136 (575,18)	2181 (0,0,39)	2183 (0,0,39)	2188 (0,0,38)	2188 (0,0,37)	2192 (0,0,37)
ν_s	1407 (2,4,0.6)	1399 (2,4,0)	1392 (2,4,0)	1385 (1,9,3.7)	1379 (0,39)	1374 (0,39)	1406 (1,3,16)	1402 (1,3,16)	1397 (0,6,25)	1390 (0,9,21)	1371 (0,3,30)	1408 (2,4,0)	1409 (2,5,0.0)	1411 (2,4,0.0)	1411 (2,6,0.0)	1412 (2,4,0.0)
ν_s	1407 (0,34)	1399 (0,36)	1392 (0,37)	1385 (0,2,34)	1379 (1,8,0)	1374 (1,6,0)	1406 (1,1,19)	1402 (1,0,20)	1397 (1,6,13)	1389 (1,1,19)	1370 (2,2,14)	1408 (0,36)	1409 (0,0,35)	1411 (0,0,36)	1411 (0,0,36)	1412 (0,0,36)
π_s	664 (0,0,8.1)	665 (0,0,8.1)	666 (0,0,7.8)	666 (0,0,7.5)	666 (0,0,7.3)	666 (0,0,7.3)	664 (0,1,8.1)	664 (0,01,8.1)	663 (0,36,7.9)	661 (0,1,7.5)	656 (0,35,4.3)	664 (0,0,7.7)	663 (0,0,6.9)	662 (0,0,5.7)	662 (0,0,5.1)	662 (0,0,3.8)
π_{as}	662 (27,0.0)	664 (23,0.0)	665 (23,0.0)	665 (21,0.0)	665 (18,0.0)	665 (16,0.0)	662 (27,0.17)	661 (26,0.48)	660 (24,1.0)	658 (23,1.4)	653 (14,1.0)	662 (28,0.0)	660 (28,0.0)	659 (28,0.0)	658 (28,0.0)	658 (26,0.0)
π_s	638 (17,0.0)	638 (17,0.0)	637 (17,0.0)	637 (17,0.0)	638 (17,0.0)	638 (16,0.0)	639 (16,0.01)	641 (15,0.03)	643 (14,0.1)	646 (12,0.2)	650 (7,1,2.3)	638 (17,0.0)	638 (17,0.0)	638 (18,0.0)	638 (18,0.0)	638 (18,0.0)
π_{as}	637 (0,1.4)	637 (0,1.4)	636 (0,1.4)	637 (0,1.4)	637 (0,1.4)	638 (0,1.5)	637 (0,2,1.4)	639 (0,5,1.2)	642 (1,3,1.0)	645 (1,6,0.8)	650 (6,7,0.7)	637 (0,0,1.4)	637 (0,0,1.5)	636 (0,0,1.7)	637 (0,0,1.8)	637 (18,0.0)

Table 8 Frequency and intensity (infrared, Raman) data for a system of two coplanar azide groups, of D_{2h} (Azide-Azide shift), D_2 (Azide-Azide torsion) and C_{2h} (Azide-Azide twist), symmetries in $Na_2(N_3)_2$ (frequencies are in cm^{-1} , infrared intensities in $KM/Mole$, Raman in $\text{\AA}^4/amu$)

In a further exploration of the effect of changes of azide geometry on frequency, we considered the case in which a D_{2h} azide symmetry was not preserved by two azides in $\text{Na}_2(\text{N}_3)_2$, only C_{2h} . The system studied was that of Figure 5 but with a sideways displacement, slip, of each azide in a direction along the N_3 axis (Figure 9). The Na..Na distance was held at 4.652\AA and the slip varied in steps of 0.2\AA . All geometries were optimised; the azide angle remained at 179° and the N-N distances changed by a maximum of 0.002\AA . The behaviour of the

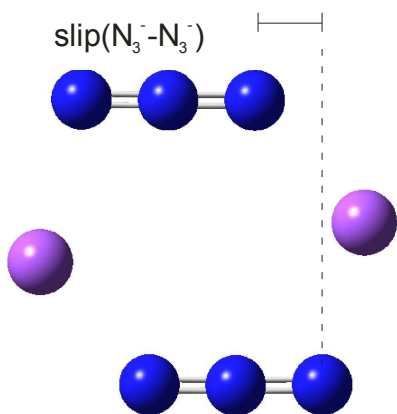


Figure 9 The arrangement of $\text{Na}_2(\text{N}_3)_2$ shown in Figure 5 but with an additional sideways slip of the azides, retaining a centre of symmetry.

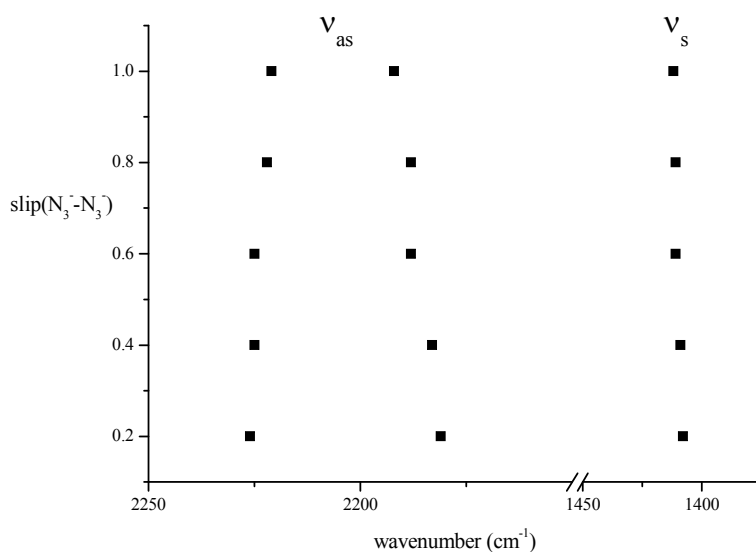


Figure 10 The variation of azide stretching mode frequencies (cm^{-1}) consequent upon slip of azide anions relative to each other in the arrangement of Figure 9

calculated frequencies is shown in Figure 10. Slip has very little effect on frequencies. A slip of 1\AA only changes the stretching mode frequencies by ca 10 cm^{-1} ; similarly the separation between the two modes increases by ca 10 cm^{-1} . These patterns will not show much spectral evidence. As for the first displacement considered above, only the higher frequency antisymmetric vibration is strong in the infrared; its lower frequency counterpart is the strongest Raman mode. The frequencies of the deformation modes of the two azides are almost independent of slip (not shown in Figure 10 but detailed in Table 8). There is one additional important feature, common to all of the cases just considered. Coupling between the azides leads to only one member of each resultant pair having significant spectral activity, with consequent apparent spectral simplification.

The above studies prompted another; to what extent is the presence of metal ion(s) – here Na^+ - essential to the calculated patterns? We therefore carried out calculations on metal-free (and external charge-free) systems. Data were obtained on two coplanar and parallel azide anions, inter-related by a mirror plane reflection but with varying separation. The data obtained are given in Table 9, which is to be compared with the data in Figure 6. The antisymmetric stretches couple, with a magnitude which decreases slowly with increased separation. However, only the higher frequency mode has any infrared activity, the lower is silent. Comparison with Figure 6 shows that both the splitting and dependence of frequency on separation are significantly enhanced by the presence of metal ions. The symmetric stretches couple but neither split nor change frequency significantly. Comparison with Figure 6 shows that the presence of metal ions does not affect this splitting, it is still zero, but does lead to a significant dependence of frequency on separation. Overall, these calculations confirm that bridge azides show a sensitivity to charge effects, just as do terminal azides.

d(az-az) (Å)	3.43	3.63	3.83	4.03	4.23	4.43	4.63	4.83
ν_{as}	2170 (1138,0)	2170 (1173,0)	2169 (1187,0)	2168 (1207,0)	2167 (1225,0)	2167 (1240,0)	2167 (1254,0)	2166 (1265,0)
	2136 (0,0.2)	2140 (0,0.2)	2144 (0,0.2)	2147 (0,0.15)	2150 (0,0.13)	2152 (0,0.12)	2153 (0,0.10)	2154 (0,0.09)
ν_{s}	1367 (0,37)	1366 (0,38)	1366 (0,39)	1366 (0,39)	1366 (0,38)	1366 (0,23)	1366 (0,28)	1366 (0,24)
	1366 (0,0)	1366 (0,0)	1366 (0,0)	1366 (0,0)	1366 (0,2.1)	1366 (0,18)	1366 (0,13)	1366 (0,18)

Table 9 The variation of azide stretching mode frequencies (cm^{-1}) with azide separation for two azides with overall D_{2h} symmetry together with spectral activities (infrared in KM/Mole , Raman in $\text{\AA}^4/\text{amu}$)

To investigate isolated azides further, and in particular the vibrational coupling between them, we have studied sets of these anions, placed as close together as is possible for stability (a c. of g. separation of 5.18 \AA was used). The detailed results are given in the Deposited Document. When the n azides were parallel to a common C_n axis, a remarkable result was obtained. With $n = 2$, antisymmetric stretching modes at 2165 and 2155 cm^{-1} were obtained. With $n = 5$ the highest frequency mode was at 2167 and the lowest at 2153 cm^{-1} . The patterns for $n = 3$ and 4 were similar; there was a splitting of $12 \pm 2 \text{ cm}^{-1}$ independent of n , weak coupling seems indicated. For all cases, the symmetric stretching modes were ostensibly uncoupled, consisting of n superimposed modes at 1365 ($n = 2$) or 1366 ($n = 3,4,5$) cm^{-1} . However, the intensities tell a different story; all of the Raman activity is confined to a single mode, that at highest frequency. Similarly, the highest frequency antisymmetric mode was the only one with infrared intensity. That is, vibrational spectroscopy is blind to the presence of multiple parallel azide groups, notwithstanding the fact that they are coupled. A very different pattern is obtained when the azide groups are co-planar. All frequencies are sensitive to n ; as n increases, so frequencies decrease. So, from $n = 3$ to 5 the highest frequency (Raman active) antisymmetric stretching mode decreases from 2105 to 2068 cm^{-1} (the degenerate, infrared active, antisymmetric stretching modes drop from 2085 to 2041 cm^{-1}). The Raman active highest frequency symmetric stretch decreases from 1322 ($n = 3$) to 1273 ($n = 5$) cm^{-1} . As n increases so the overall frequency range increases. So, for $n = 3$, the spread of asymmetric frequencies is 22

cm^{-1} but for $n = 5$ it is 55 cm^{-1} . The symmetric stretch behaves similarly, but with a smaller spread. The conclusion is clear. Both parallel and co-planar azide anions interact vibrationally, even when physically well separated. Whilst that between parallel azides is essentially constant, that between co-planar azides varies considerably.

All of the above work refers either to individual azides or to sets, the members of which are symmetry-related. We have also studied two systems with symmetry distinct species, one with two and the other with three different azides; both are copper systems, one Cu^+ (C_s symmetry), the other Cu^{2+} (C_{2h} symmetry). They are shown in Figure 11, where the optimized geometries are given. The results are detailed in Table 10. It is evident that zeroth-order frequencies are important. Only the vibrations of symmetry-related azide groups couple. So, in the Cu^+ species, B and B' couple - but there is no significant coupling between A and A' or between either A and the B's. Although the coupling may lead to a small splitting, always less than 10 cm^{-1} , it can lead to a total transfer of spectral intensity. So, for the Cu^{2+} species each mode has a zero intensity for one activity. This, of course, is nothing more than the consequence of the centre of symmetry, but the pattern for the Cu^+ compound is not dissimilar and in it may lie the, otherwise surprising, different activities of the two highest frequency modes of this compound.

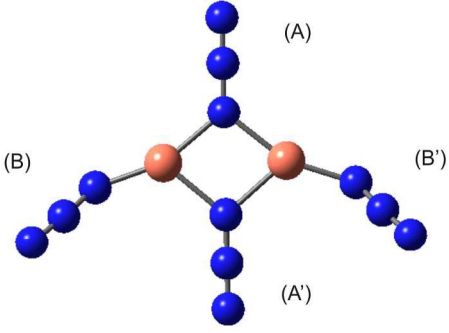
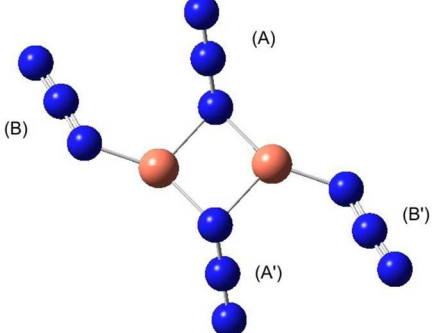
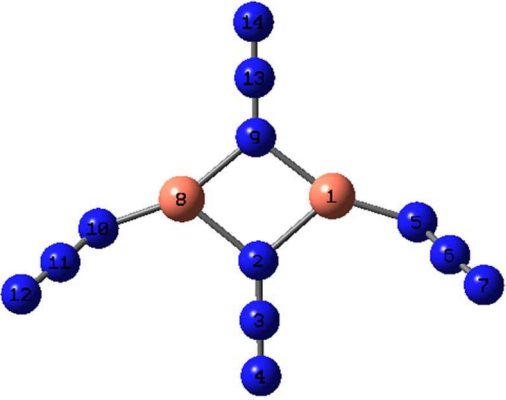
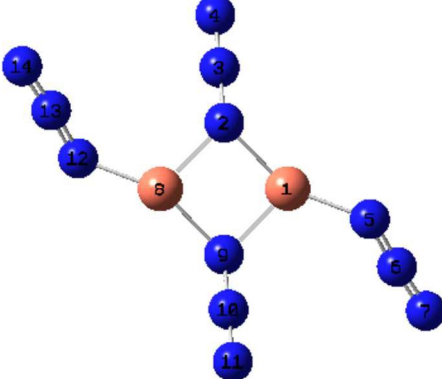
$[\text{Cu}_2(\mu_2\text{-N}_3)_2(\text{N}_3)_2]^{2-}$; Cu(I)	$\text{Cu}_2(\mu_2\text{-N}_3)_2(\text{N}_3)_2$; Cu(II)
	
Azides (A) and (A') are coplanar, likewise (B) and (B'); $\tau_{(A)/(B)}=110^\circ$; $\alpha(\text{N-N-Cu})_{(B)}=138^\circ$	Azides (A) and (A') are parallel but not coplanar. Azides (B) and (B') are coplanar. $\tau_{(A)/(B)}=46^\circ$; $\alpha(\text{N-N-Cu})_{(B)}=132^\circ$
	
$d(\text{Cu}1\text{-N}9) = d(\text{Cu}8\text{-N}9) = 1.985$ $d(\text{Cu}1\text{-N}2) = d(\text{Cu}8\text{-N}2) = 2.026$ $d(\text{Cu}1\text{-N}5) = d(\text{Cu}8\text{-N}10) = 1.827$ $d(\text{N}9\text{-N}13) = 1.226$; $d(\text{N}13\text{-N}14) = 1.136$ $d(\text{N}2\text{-N}3) = 1.228$; $d(\text{N}3\text{-N}4) = 1.137$ $d(\text{N}10\text{-N}11) = d(\text{N}5\text{-N}6) = 1.205$ $d(\text{N}11\text{-N}12) = d(\text{N}6\text{-N}7) = 1.147$ $d(\text{Cu}1\text{-Cu}8) = 3.102$	$d(\text{Cu}1\text{-N}2) = d(\text{Cu}8\text{-N}9) = 1.935$ $d(\text{Cu}8\text{-N}2) = d(\text{Cu}1\text{-N}9) = 2.021$ $d(\text{Cu}1\text{-N}5) = d(\text{Cu}8\text{-N}12) = 1.842$ $d(\text{N}2\text{-N}3) = d(\text{N}9\text{-N}10) = 1.228$ $d(\text{N}3\text{-N}4) = d(\text{N}10\text{-N}11) = 1.135$ $d(\text{N}5\text{-N}6) = d(\text{N}12\text{-N}13) = 1.208$ $d(\text{N}6\text{-N}7) = d(\text{N}13\text{-N}14) = 1.146$ $d(\text{Cu}1\text{-Cu}8) = 2.658$

Figure 11 Species containing symmetry non-related azides (distances are in Å, angles in degrees).

	Freq (IR, Raman)	analysis of normal modes			Freq (IR, Raman)	analysis of normal modes
ν_{as}	2187 (671, 1036)	(A)		ν_{as}	2193 (0, 1179)	(A)-(A')
ν_{as}	2134 (457, 296)	(A')		ν_{as}	2190 (1375, 0)	(A)+(A')
ν_{as}	2123 (575, 2489)	(B)+(B')		ν_{as}	2117 (0, 2684)	(B)-(B')
ν_{as}	2116 (1343, 881)	(B)-(B')		ν_{as}	2114 (1525, 0)	(B)+(B')
ν_s	1394 (54, 4)	(B)+(B')		ν_s	1377 (0, 15)	(B)+(B')
ν_s	1393(126, 0.1)	(B)-(B')		ν_s	1376 (174, 0)	(B)-(B')
ν_s	1315 (124, 37)	(A)		ν_s	1316 (0, 15)	(A)+(A')
ν_s	1277 (130, 48)	(A')		ν_s	1309 (249, 0)	(A)-(A')
π	730 (1, 0.6)	(A)		π	635 (33, 0)	[(B)+(B')]-[(A)+(A')]
π	689 (0.3, 0.7)	(A')		π	631 (0, 25)	[(B)-(B')]-[(A)-(A')]
π	621 (9, 15)	(B)+(B')		π	626 (0, 4)	[(A)-(A')]+[(B)-(B')]
π	619 (16, 3)	(B)-(B')		π	619 (11, 0)	[(A)+(A')]+[(B)+(B')]
π	593 (4, 1)	(A)		π	601 (0, 22)	(A)-(A')
π	586 (6, 0.6)	(A')		π	597 (14, 0)	(A)+(A')
π	567 (14, 2)	(B)+(B')		π	577 (9, 0)	(B)+(B')
π	567 (4, 1)	(B)-(B')		π	577 (0, 4)	(B)-(B')

Table 10 Frequency and spectral activity data for the azide vibrational modes of the two model species shown in Figure 11; Cu⁺ left, Cu²⁺ right. Here, A and B refer to the azide groups of

Figure 11 (upper) and so enable the parentage of mixed modes to be determined (frequencies are in cm^{-1} , infrared in KM/mole , Raman in $\text{\AA}^4/\text{amu}$).

The last study that we have made concerns the vibrational consequences of adding further simple ligands to the system. The species studied and the results are given in Table 11. The species are given in more detail in the Deposited Document. The cyanide anion has been chosen for Ni^{2+} , Zn^{2+} (in both cases with three cyanides but only one azide) and Cu^+ . Cu^+ with NH_3 as co-ligand has also been studied. Included in the Table are data on Cu^{2+} with Cl^- and Br^- as co-ligands. They differ little from those involving Cu^+ . Formal valence states are perhaps less important than formal charge. The results testify to the unpredictability of azide as a ligand. So, although $[\text{NiN}_3]^-$ has its antisymmetric stretching mode at 2086 cm^{-1} and that of $[\text{Ni}(\text{CN})_3\text{N}_3]^{2-}$ is at 2147 cm^{-1} , the data for the corresponding Zn^{2+} species are 2154 and 2157 cm^{-1} respectively. In contrast, the frequency change on the symmetric stretch is the greater for the zinc species (159 as compared to 103 cm^{-1}). For the (split) deformation modes, one increases and one decreases in frequency for Ni^{2+} whilst for Zn^{2+} both increase. For Cu^+ the picture is much simpler. All of the additional ligands that we have studied lead to an increase in frequency of both symmetric and antisymmetric azide vibrational frequencies. The deformations behave less regularly but the frequency changes are not great, maximum values were 13 and 24 cm^{-1} . Three of the molecules in Table 11 contain both CN^- and N_3^- , ions which might be expected to couple vibrationally. In the Ni complex, there is a weak coupling between all of the cyanide modes and the azide antisymmetric stretch; the mixing with the totally symmetric cyanide mode ($\nu_{\text{CN}} = 0 \text{ cm}^{-1}$) is the

greatest but remains very small. For the corresponding Zn complex the coupling pattern is similar but even smaller ($\nu_{\text{CN}} = 2216\text{cm}^{-1}$). Even for the Cu complex, where the anions are almost co-linear, the coupling is small ($\nu_{\text{CN}} = 2273\text{cm}^{-1}$). These results probably serve to remove one ambiguity. When the azide anion is coordinated together with other ligands with which it might vibrationally couple, this coupling can normally be ignored.

	Ni(II)Az	[Ni(CN) ₃ Az] ²⁻	Zn(II)Az	[Zn(CN) ₃ Az] ²⁻	Cu(I)Az	[CuCNAz] ⁻	CuNH ₃ Az	CuClAz	CuBrAz
ν_{as}	2086	2147	2154	2157	2165	2185	2196	2174	2173
ν_{s}	1295	1398	1239	1398	1345	1412	1392	1400	1398
π	594	659	620	654	649	636	651	640	641
π	476	322	527	628	575	599	587	598	598
	443	614	429	282	444	470	499	425	408
	113	190	183	130	145	131	166	149	137
$q_{(\text{M})}$	1.020	-0.061	1.329	0.654	0.687	0.450	0.560	0.491	0.464
$q_{(\text{N1})}$	-0.412	-0.400	-0.634	-0.519	-0.687	-0.602	-0.653	-0.600	-0.502
$q_{(\text{N2})}$	0.180	0.200	0.178	0.199	0.186	0.200	0.201	0.194	0.194
$q_{(\text{N3})}$	0.212	-0.427	0.127	-0.445	-0.186	-0.361	-0.250	-0.374	-0.370
M-N-N	141	138	120	138	124	141	132	137	137
N-N-N	175	175	171	177	174	176	176	176	176
d(M-N)	1.733	1.950	1.872	2.080	1.845	1.868	1.829	1.870	1.874

Table 11 DFT results for $[\text{MN}_3]^{\text{n}+}$ and related mixed-ligand complexes.

Conclusions

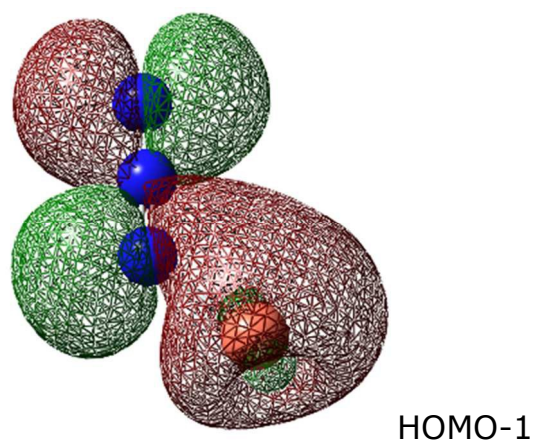
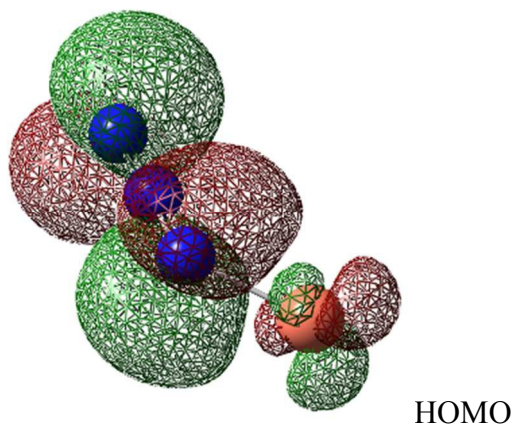
The motivation for the present study was an attempt to understand the apparent lack of correlation between geometric environment and vibrational characteristics of the azide anion. Whilst our conclusion is that no immediate correlation is to be expected, we believe that a much better understanding has emerged. Firstly, proximate azide groups are normally vibrationally coupled. This coupling is probably dipolar in nature and it attenuates as the molecular complexity increases. The existence of this coupling means that the vibrational spectra might reasonably be expected to be good indicators of molecular geometry. There are two features mitigating against this indication. First, azide vibrations are sensitive to the polar, dipolar and quadrupolar nature of their local environment. This means that the observed frequency is not a unique indicator of coordination geometry in the same way that it is for the coordinated CO group. Both CO and N_3^- show vibrational coupling but the charge on the azide ion makes its observed frequencies almost useless as indicators. The second problem is that of intensities. When, for instance, the azide antisymmetric stretch is split, almost all of the infrared intensity is concentrated in a single component unless the molecular symmetry is very low. Simple group-theoretical analyses coupled with band counting will not give molecular geometries, again a difference from the CO ligand. Reports of Raman studies are rare and perhaps our calculations explain why. The symmetric stretch mode of the coordinated azide group has a surprisingly low Raman intensity and a reliable assignment of it in the presence of additional ligands of any complexity is improbable. Also surprisingly, it would seem that a formally infrared active, but

essentially silent, antisymmetric stretching mode may reveal its presence in a Raman spectrum, sometimes having a greater intensity than the symmetric components combined.

Finally, it possible to suggest the way forward to a better understanding of the vibrational spectra of the azide ligand. Firstly, it would normally be sensible to ignore the actual observed frequencies (the exception is when closely related compounds are involved). The general pattern is of more significance. Secondly, combined infrared and Raman data may enable the use of a simple group-theoretical analysis in the 2100 cm^{-1} region. Infrared data alone are unlikely to be sufficient. Thirdly, whilst the 1400 cm^{-1} region should be studied, it is probable that only in those cases where an understanding of the antisymmetric stretch region has already been achieved that such a study will itself give useful data. However, our, pessimistic, general conclusion is that vibrational spectroscopy will seldom give reliable insights into the geometric disposition of azide groups within a complex, unless it be for a set of closely related compounds.

Appendix.

The Figure shows the HOMO and HOMO-1 in the Cu(I)-azide system, which is calculated to be bent with a N-N-Cu angle of 124° . Whilst the HOMO shows a π interaction between Cu and terminal nitrogen, this has both bonding and antibonding components. It would seem equally appropriate for a linear molecule; certainly, it offers no explanation for the greater stability of a bent. The most important contributor to this preference is HOMO-1. It has a dominant Cu σ interaction with one lobe of a N-N π bonding orbital.



FOOTNOTES

Corresponding Author

Eliano Diana, Dipartimento di Chimica, Università di Torino, via P. Giuria 7, 10125 Torino,

Italy; e-mail: eliano.diana@unito.it; tel. +39 011 6707572; fax +39 011 6707855

REFERENCES

- (1) Leibelng, G., Demeshko, S., Bauer-Siebenlist, B., Meyer, F., Pritzkow, H. *Eur. J. Inorg. Chem.* 2004, 2413–2420.
- (2) Agrell, I. *Acta Chemica Scand.* 1971, **25**, 2965-2974
- (3) Gray, P., Waddington, T. C. *Trans. Faraday Soc.* 1957, **53**, 901-908.
- (4) Dori, Z., Ziolo R. F. *Chem. Rev.* 1973, **73**, 247-254
- (5) Mautner F. A., Louker F. R., Hofer J., Spell M., Lefèvre A., Guilbeau A. E., Massoud S. S. *Cryst. Growth Des.* 2013, **13**, 4518–4525
- (6) Nakamoto K. *Infrared and Raman spectra of inorganic and coordination compounds*, John Wiley & Sons, New York, 1986.
- (7a) Kettle, S. F. A., Diana, E., Marchese, E. M. C., Boccaleri, E., Croce, G., Sheng, T., Stanghellini, P. L. *Eur. J. Inorg. Chem.* 2010 3920–3929.
- (7b) Kettle S.F.A., Aschero G.L., Diana E., Rossetti R., Stanghellini P.L. *Inorg Chem.* 2006, **45**, 4928-4937.
- (7c) Kettle S.F.A., Diana E., Boccaleri E., Stanghellini P.L. *Inorg Chem.* 2007, **46**, 2409-2416
- (8a) Schulz A., Tornieporth-Oetting I. C., Klapotke T. M. *Inorg. Chem.* 1995, **34**, 4343-4346
- (8b) Kandalam A. K., Blanco M. A., Pandey R. *J. Phys. Chem. B* 2001, **105**, 6080-6084
- (8c) Jensen J. O. *Spectrochimica Acta Part A* 2003, **59**, 2805-2814

- (8d) Haiges R., Boatz J. A., Schneider S., Schroer T., Yousufuddin M., Christe K. O. *Angew. Chem. Int. Ed.* 2004, **43**, 3148–3152
- (8e) Qian Shu Li, Hong Xia Duan *J. Phys. Chem. A* 2005, **109**, 9089-9094
- (8f) Haiges R., Boatz J. A., Bau R., Schneider S., Schroer T., Yousufuddin M., Christe K. O. *Angew. Chem. Int. Ed.* 2005, **44**, 2–6
- (8g) Ogden J. S., Dyke J. M., Levason W., Ferrante F., Gagliard L. *Chem. Eur. J.* 2006 , **12**, 3580-3586
- (8h) Afyonb S., Höhna P., Armbrüster M., Baranova A., Wagner F. R., Somerb M., Kniepa R. *Z. Anorg. Allg. Chem.* 2006, **632**, 1671-1680
- (8i) Haiges R., Boatz J. A., Schroer T., Yousufuddin M., Christe K. O. *Angew. Chem. Int. Ed.* 2006, **45**, 4830-4835
- (8j) Haiges R., Boatz J. A., Christe K. O. *Angew. Chem. Int. Ed.* 2010, **49**, 8008-8012
- (8k) Schulz A., Villinger A. *Chem Eur J.* 2012, **18**, 2902-2911
- (8l) Villinger A., Schulz A. *Angew. Chem. Int. Ed.* 2010, **49**, 8017–8020
- (8m) Rosenstengel K., Schulz A., Villinger A. *Inorg. Chem.* 2013, **52**, 6110–6126.
- (8n) Haiges R., Rahm M., Dixon D. A., Garner E. B., Christe K. O. *Inorg. Chem.* 2012, **51** 1127–1141
- (8o) Lyhs B., Bläser D., Wölper C., Schulz S., Haack R., Jansen G. *Inorg. Chem.* 2013, **52** 7236–7241

- (8p) Haiges R., Rahm M., Christe K. O. *Inorg. Chem.* 2013, **52**, 402–414
- (8q) Shaabani B., Mirtamizdoust B., Shadman M., Hoong Kun Fun Z. *Anorg. Allg. Chem.* 2009, **635**, 2642–2647
- (8r) Lyhs B., Bläser D., Wölper C., Schulz S., Jansen G. *Inorg. Chem.* 2012, **51**, 5897–590
- (8s) Lund, H., Oeckler, O., Schröder, T., Schulz, A., Villinger, A. *Angew. Chem. Int. Ed.* 2013, **52**, 10900–10904.
- (8t) Klapötke T. M., Schulz A. *Structural Chemistry* 1997, **8 (6)**, 421-423
- (8u) Schulz A., Klapötke T. M. *Inorganic Chemistry* 1997, **36**, 1929-1933
- (8v) Klapötke T. M. *Chemische Berichte* 1997, **130 (4)**, 443-452
- (8w) Klapötke T. M., Schulz A. *Inorg. Chem.* 1996, **35**, 4995–4998
- (8x) Fan Y., Hall M.B. *Chem. Eur. J.* 2004, **10**, 1805-1814
- (9) Frisch, M. J. et al. *Gaussian 09*, Revision A.01, Gaussian, Inc.:Wallingford, CT, 2009.
- (10a) Griffi J. F., Coppens P. *J. Chem. Soc. D* 1971, 502-503
- (10b) Reckeweg O., Simon A. *Z. Naturforsch* 2003, **58b**, 1097-1104
- (11) Massoud S.S., Mautner F.A., Abu-Youssef M.A.M., Shuaib N.M., *Polyhedron* 1999, **18** 2061-2067
- (12a) Zbiri M., Saha S., Adhikary, C., Chaudhuri S., Daul C., Koner S., *Inorg. Chim. Acta* 2006, **359**, 1193-1199

(12b) Shi-Qiang Bai, En-Qing Gao, Zheng He, Chun-Hua Yan *New J. Chem.* 2005, **29**, 935-941

(12c) W. Dong, Y. Ouyang, D-Z. Liao, S-P. Yan, P. Cheng, Z-H. Jiang *Inorg. Chim. Acta* 2006, **359**, 3363-3366

(12d) Ghoshal D., Maji T.K., Rosair G., Mostafa G. *Acta Cryst C* 2004, **C60**, m212-m214

(12e) Chattopadhyay S., Ray M.S., Drew M.G.B., Figuerola A., Diaz C., Ghosh A. *Polyhedron* 2006, **25**, 2241-2253

(13) Massoud S.S., Mautner F.A. *Inorg. Chim. Acta* 2005, **358**, 3334-3340

(14) Abu-Youssef M.A.M., Escuer A., Goher M.A.S., Mautner F.A., Vicente R. *Eur. J. Inorg. Chem.* 1999, 687-691





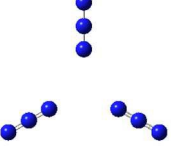
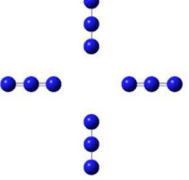
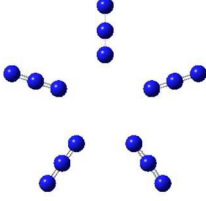
ELECTRONIC SUPPLEMENTARY INFORMATION

S1: Vibrational interaction between isolated azides

S2: Details of the species given in Table 11

S1 Sets of symmetry-related azide groups (2 to 5) either parallel or perpendicular, subject to various displacements, together with the calculated vibrational frequencies and activities. A c. of g. separation of 5.18 Å was used throughout.

	2	3	4	5
--	---	---	---	---

				
ν_{as}	2165 (vs,0) 2155 (0)	2167 (vs,0) 2153 (0, vw) 2153 (0,vw)	2166 (vs,0) 2154 (0,vw) 2154 (0,vw) 2147 (0,0)	2167 (vvs,0) 2159(0,vw) 2159 (0,vw) 2153 (0,0) 2153 (0,0)
ν_s	1365(0,0) 1365(0,m)	1366 (0,m) 1366 (0,0) 1366 (,0)	1366 (0,m) 1366 (0,0) 1366 (0,0) 1366 (0,0)	1366 (0,m) 1366 (0,0) 1366 (0,0) 1366 (0,0) 1366 (0,0)
				
ν_{as}		2119 (w,m) 2103 (vs,w) 2103 (vs,w)	2095 (0,m) 2072 (s,0) 2072 (s,0) 2060 (0,w)	2100 (0,m) 2079 (vs,0) 2079 (vs,0) 2061 (0,vvw) 2061 (0,vvw)
ν_s		1329 (0,vs)	1303 (0,s)	1298 (0,vs)

		1328 (w,s)	1298 (m,0)	1294 (m,0)
		1328 (w,s)	1298 (m,0)	1294 (m, 0)
			1295 (0,m)	1290 (0,w)
				1290 (0,w)

S2 Details of the species given in Table 11

Ni(II)Az	$[\text{Ni}(\text{CN})_3\text{Az}]^{2-}$	Zn(II)Az
$[\text{Zn}(\text{CN})_3\text{Az}]^{2-}$	Cu(I)Az	$[\text{Cu}(\text{CN})\text{Az}]^-$
Cu(NH ₃)Az	CuClAz	CuBrAz

